Electronic Supplementary Material (ESI) for Dalton Transactions.
This journal is © The Royal Society of Chemistry 2023

Controlled synthesis of M doped NiVS (M=Co, Ce and Cr) as robust electrocatalyst for urea electrolysis

Chao Wang[a], Qirun Wang[a], Xiaoqiang Du[a*] and Xiaoshuang Zhang[b]

[a] School of Chemistry and Chemical Engineering , North University of China, Xueyuan road 3, Taiyuan 030051, People's Republic of China. E-mail: duxq16@nuc.edu.cn

[b] School of Environment and Safety Engineering, North University of China, Xueyuan road 3, Taiyuan 030051, People's Republic of China.

DFT computation details: The DFT calculations were performed using the Cambridge Sequential Total Energy Package (CASTEP) with the plane-wave pseudo-potential method. The geometrical structures of the (110) and (011) plane of NiS and VS_4 was optimized by the generalized gradient approximation (GGA) methods. The Revised Perdew-Burke-Ernzerh of (RPBE) functional was used to treat the electron exchange correlation interactions. A Monkhorst Pack grid k-points of 6*6*1 and 5*2*1 of NiS and VS_4, a plane-wave basis set cut-off energy of 500 eV were used for integration of the Brillouin zone. The structures were optimized for energy and force convergence set at 0.05 eV/A and 2.0×10^{-5} eV, respectively. The Gibbs free energy of H adsorption was calculated as follows:

$$\Delta G_{H*} = \Delta E_{H*} + \Delta ZPE - T\Delta S$$

Where ΔZPE is the zero-point energy and TΔS stands for the entropy corrections. According to the previous report by Norskov et al., we used the 0.24 eV for the ΔZPE - TΔS of hydrogen adsorption in this work.

Res: J. Electrochem. Soc., **2005**, 152, J23.

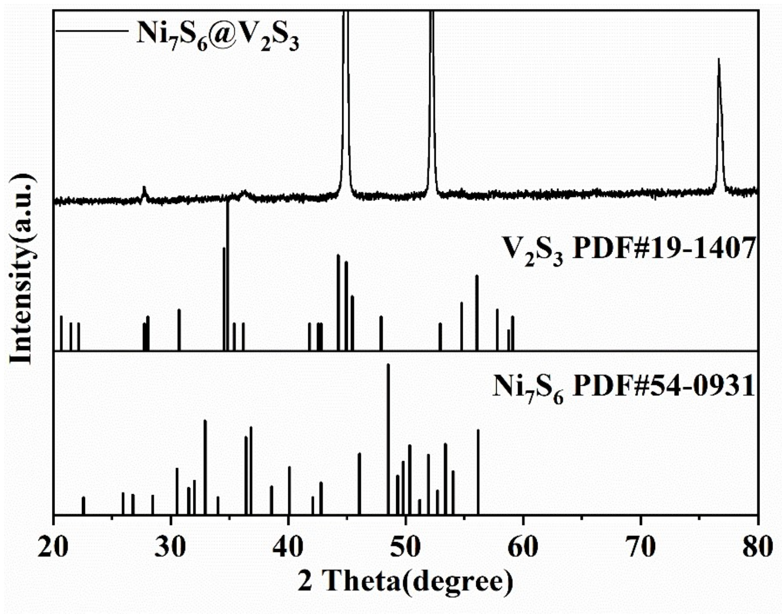

Fig. S1. XRD of NiVS.

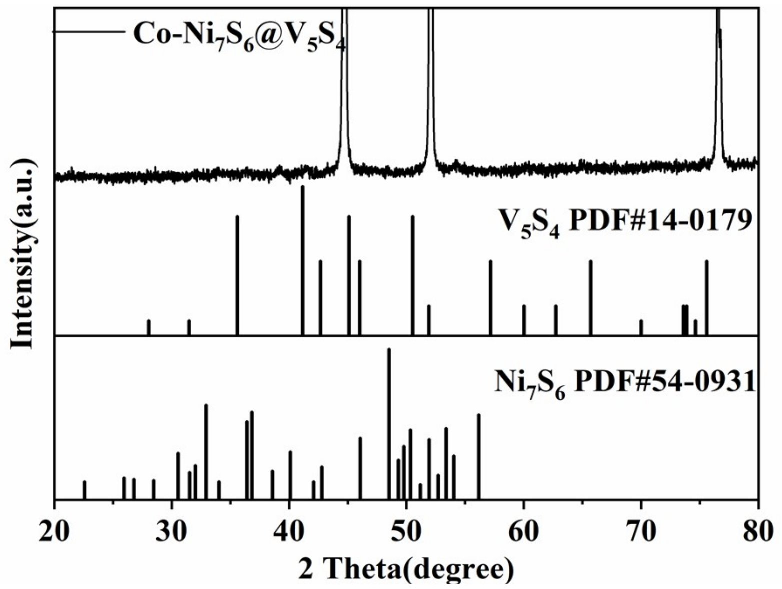

Fig. S2 XRD of Co-NiVS.

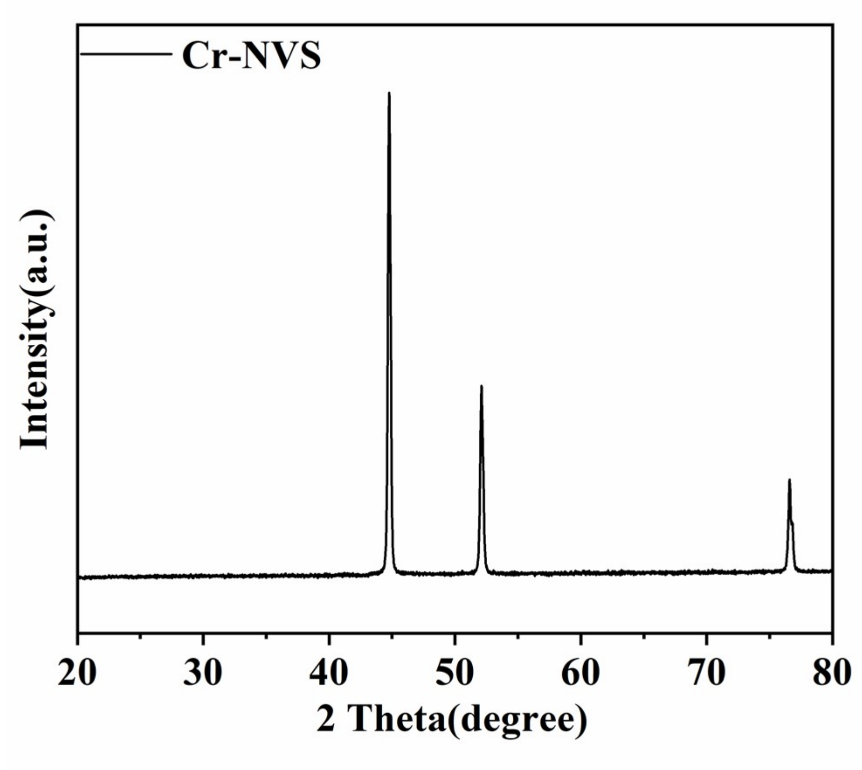

Fig. S3 XRD of Cr-NiVS.

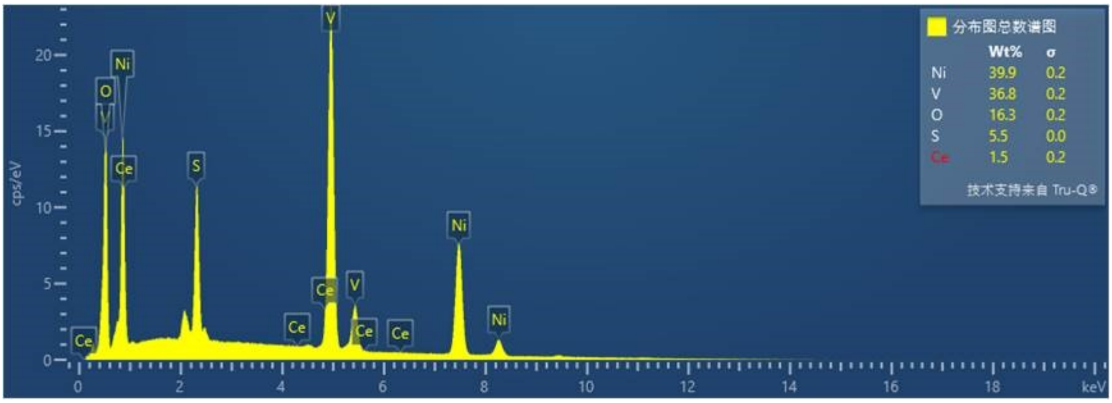

Fig. S4 Quantitative analysis of EDS characterization of Ce-NiVS catalyst.

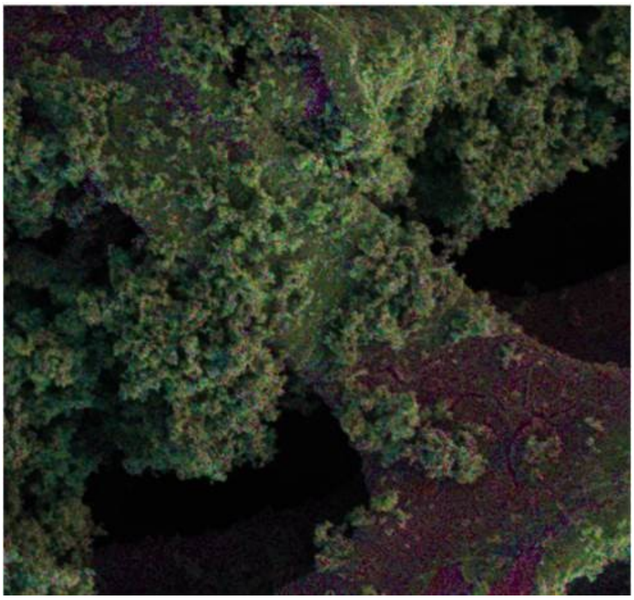

Fig. S5 EDS layered images.

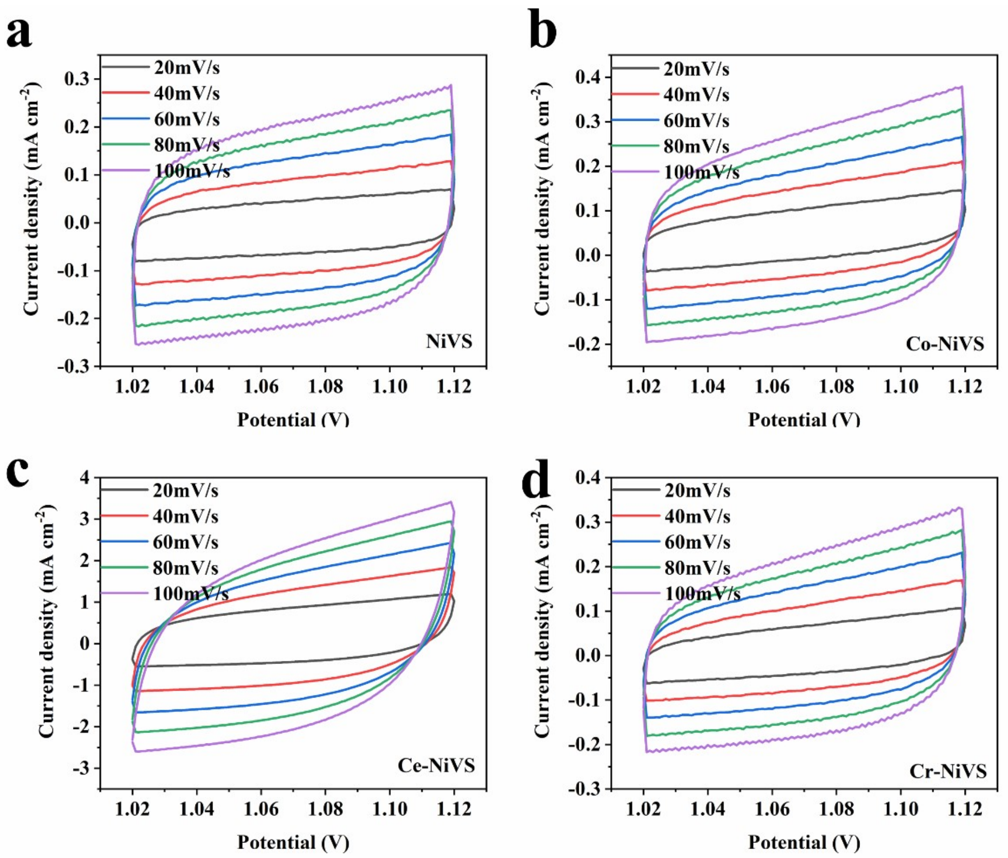

Fig. S6. CV curves of UOR: (a) NiVS, (b) Co-NiVS, (c) Ce-NiVS, (d) Cr-NiVS.

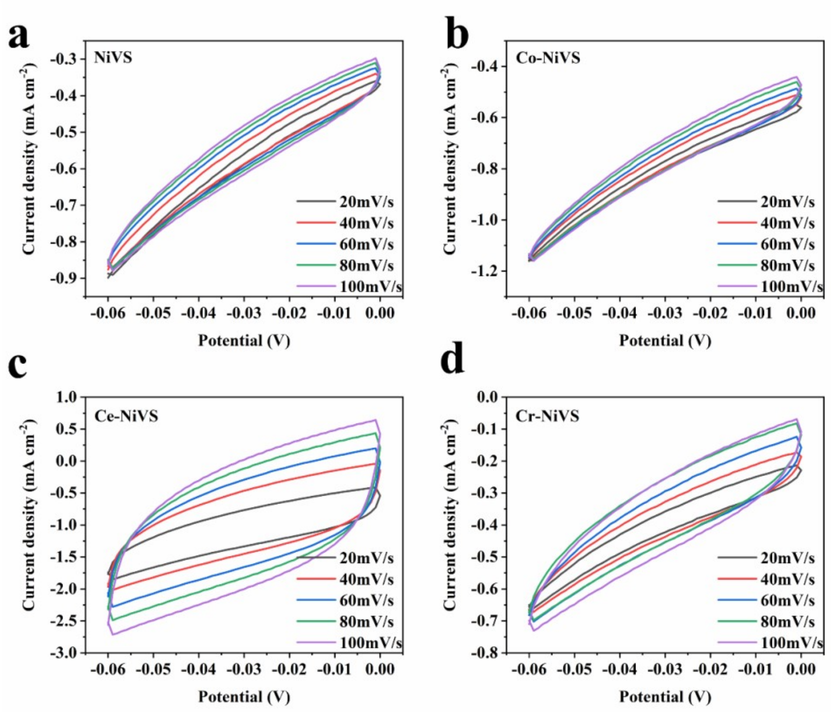

Fig. S7. CV curves of HER: (a) NiVS, (b) Co-NiVS, (c) Ce-NiVS, (d) Cr-NiVS.

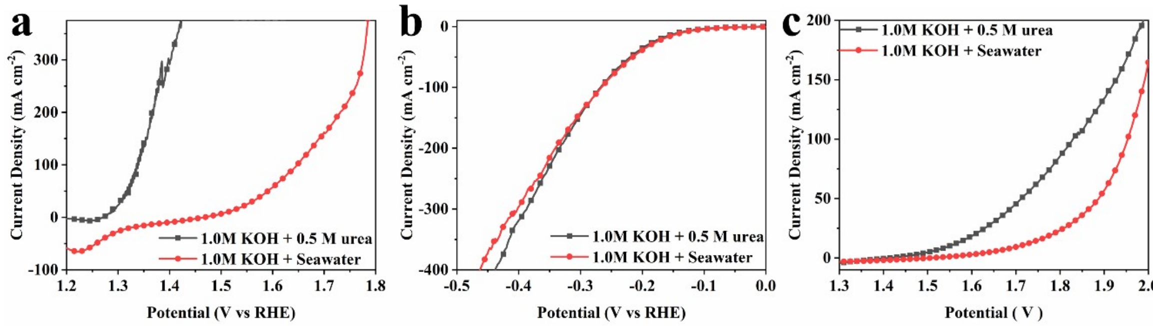

Fig. S8. Comparison of the properties of Ce-NiVS catalysts in alkaline urea and alkaline seawater: (a) anode reaction, (b) cathode reaction, (c) total hydrolysis.

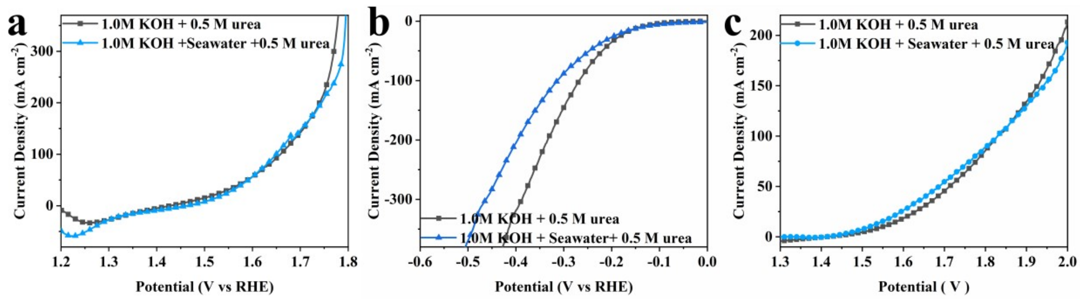

Fig. S9. Comparison of the properties of Ce-NiVS catalysts in alkaline urea and alkaline urea seawater: (a) anode reaction, (b) cathode reaction, (c) total hydrolysis.

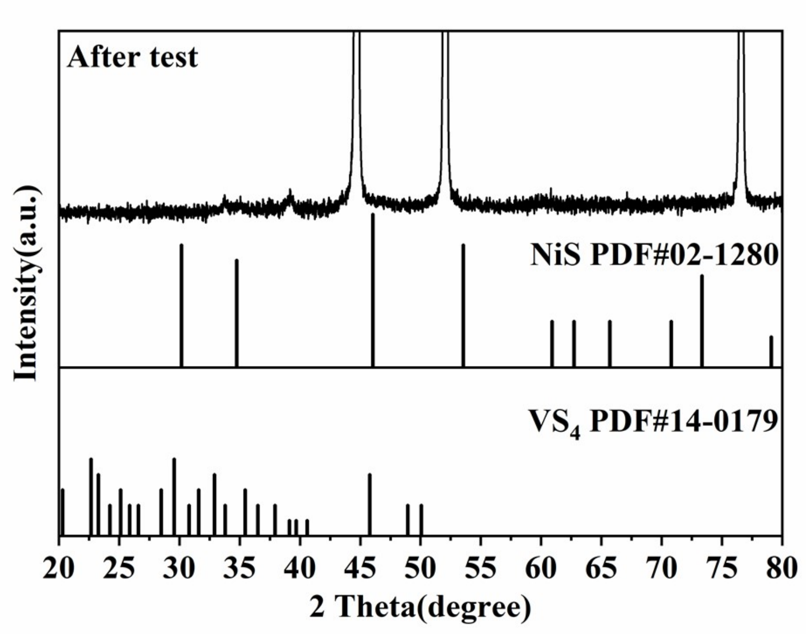

Fig. S10.XRD image of Ce-NiVS catalyst after stability test.

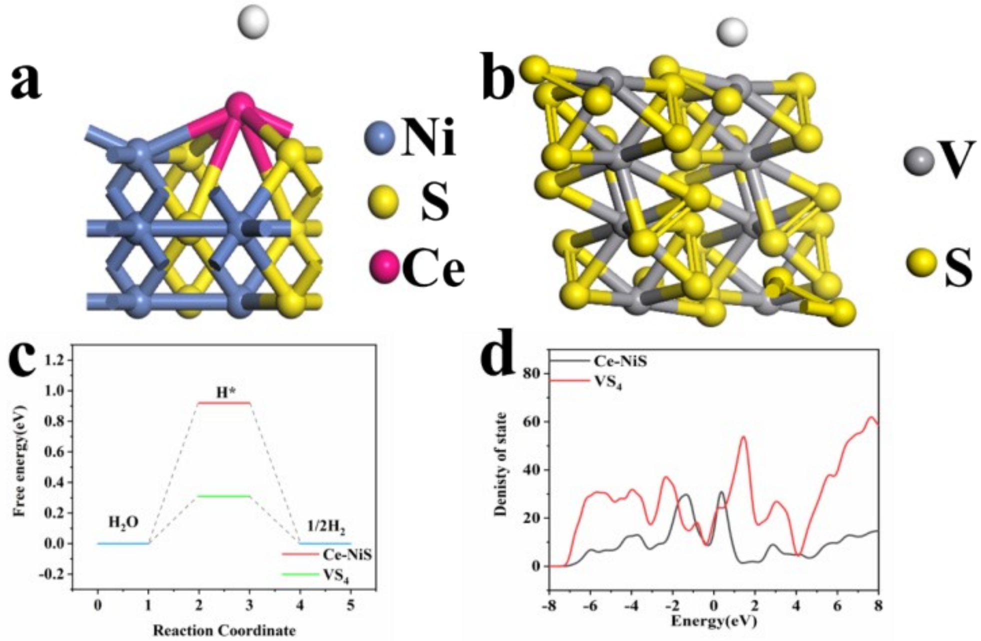

Fig. S11 (a-b) Adsorption models of H* on Ce-NiS and VS_4, (c) obtained free energy diagram for HER, (d) obtained H* state densities of Ce-NiS and VS_4.

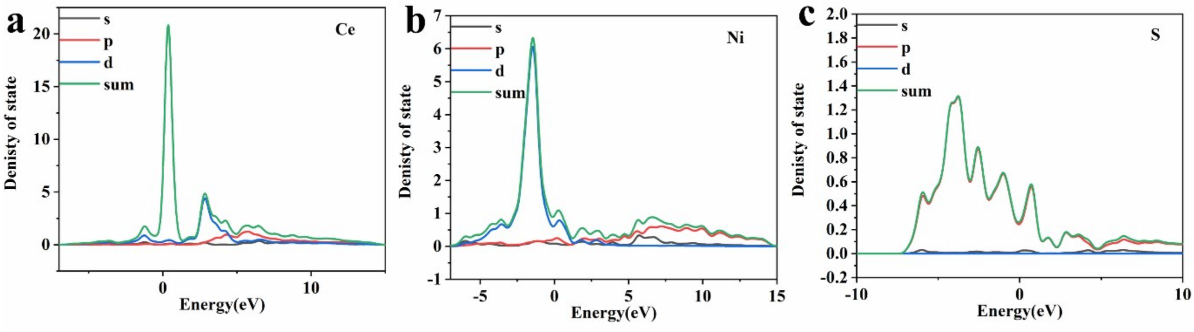

Fig. S12. Density of states for Ce-NiS, (a) Ce, (b) Ni, (c)S.

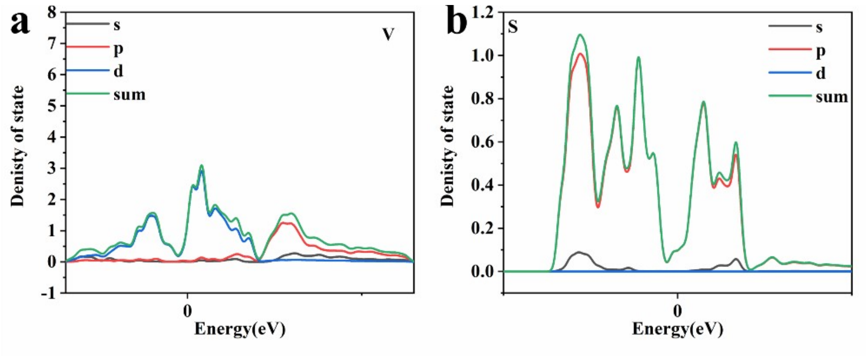

Fig. S13. Density of states for VS_4, (a)V, (b) S.

Table S1. Comparison of this work for UOR in 1.0 M KOH with 0.5 M urea solution with other works

Catalyst	j / mA cm^{-2}	Voltage / V	Reference
Ce-NiVS	10	1.29	This work
$NiMoO_4$	10	1.37	[1]
CoS_2/Ti mesh	10	1.40	[2]
NiMo@ZnO/NF	10	1.405	[3]
Ni_2P/CFC	10	1.42	[4]
$Ni(OH)_2$ nanotube-NF	10	1.41	[5]
NiCo alloy	10	1.53	[6]

Table S2. Comparison of the HER performance for Ce-NiVS catalyst with other reported catalysts in alkaline solution

Catalyst	j / mA cm^{-2}	Overpotential / mV	Reference
Ce-NiVS	10	141	This work
NiCo/NiCoO$_x$	10	155	[7]
CoO$_x$@CN	10	232	[8]
Co$_9$S$_8$@NiCo LDH	10	168	[9]
Co-Ni$_3$N	10	180	[10]
MoS$_2$/NiCoS	10	189	[11]
MoO$_3$-MoS$_2$/FTO	10	310	[12]
Co$_{0.6}$Mo$_{1.4}$N$_2$	10	200	[13]

Table S3. Comparison of the performance of urea electrolysis for Ce-NiVS catalyst with other reported catalysts in alkaline solution

Catalyst	potential (V at 10 mA cm^{-2})	Electrolyte	Reference
Ce-NiVS	1.50	1.0 MKOH+ 0.5M urea	This work
MnO$_2$/MnCo$_2$O$_4$	1.58	1.0 MKOH+ 0.5M urea	[14]
NP-Ni$_{0.70}$Fe$_{0.30}$	1.55	1.0 MKOH+ 0.33M urea	[15]
Pt/C‖IrO$_2$	1.72	1.0 MKOH+ 0.5M urea	[16]
CoS$_2$/Ti mesh	1.59	1.0 MKOH+ 0.3M urea	[2]
Ni-WxC/CNTs‖WxC/ CNTs	1.65	1.0 MKOH+ 0.33M urea	[17]

Reference

[1] Z.-Y. Yu, C.-C. Lang, M.-R. Gao, Y. Chen, Q.-Q. Fu, Y. Duan, S.-H. Yu, Ni-Mo-O nanorod-derived composite catalysts for efficient alkaline water-to-hydrogen conversion via urea electrolysis;Energy Environ. Sci., 2018;11: 1890-7.

[2] S. Wei, X. Wang, J. Wang, X. Sun, L. Cui, W. Yang, Y. Zheng, J. Liu, CoS_2 nanoneedle array on Ti mesh: A stable and efficient bifunctional electrocatalyst for urea-assisted electrolytic hydrogen production;Electrochim. Acta, 2017;246: 776-82.

[3] J. Cao, H. Li, R. Zhu, L. Ma, K. Zhou, Q. Wei, F. Luo, Improved hydrogen generation via a urea-assisted method over 3D hierarchical NiMo-based composite microrod arrays;J. Alloys Compd., 2020;844: 155382.

[4] X. Zhang, Y. Liu, Q. Xiong, G. Liu, C. Zhao, G. Wang, Y. Zhang, H. Zhang, H. Zhao, Vapour-phase hydrothermal synthesis of Ni_2P nanocrystallines on carbon fiber cloth for high-efficiency H-2 production and simultaneous urea decomposition;Electrochim. Acta, 2017;254: 44-9.

[5] R.-Y. Ji, D.-S. Chan, J.-J. Jow, M.-S. Wu, Formation of open-ended nickel hydroxide nanotubes on three-dimensional nickel framework for enhanced urea electrolysis;Electrochem. Commun., 2013;29: 21-4.

[6] W. Xu, H. Zhang, G. Li, Z. Wu, Nickel-cobalt bimetallic anode catalysts for direct urea fuel cell;Scientific Reports, 2014;4: 5863.

[7] X. Yan, K. Li, L. Lyu, F. Song, J. He, D. Niu, L. Liu, X. Hu, X. Chen, From Water Oxidation to Reduction: Transformation from $NixCo_{3-x}O_4$ Nanowires to NiCo/NiCoOx Heterostructures;ACS Appl. Mater. Interfaces, 2016;8: 3208-14.

[8] H. Fei, J. Dong, M.J. Arellano-Jimenez, G. Ye, N.D. Kim, E.L.G. Samuel, Z. Peng, Z. Zhu, F. Qin, J. Bao, M.J. Yacaman, P.M. Ajayan, D. Chen, J.M. Tour, Atomic cobalt on nitrogen-doped graphene for hydrogen generation;Nat. Commun., 2015;6: 8668.

[9] C. Qin, A. Fan, X. Zhang, S. Wang, X. Yuan, X. Dai, Interface engineering: few-layer MoS_2 coupled to a NiCo-sulfide nanosheet heterostructure as a bifunctional electrocatalyst for overall water splitting;J. Mater. Chem. A, 2019;7: 27594-602.

[10] S. Deng, Y. Zhong, Y. Zeng, Y. Wang, X. Wang, X. Lu, X. Xia, J. Tu, Hollow $TiO_2@Co_9S_8$

Core-Branch Arrays as Bifunctional Electrocatalysts for Efficient Oxygen/Hydrogen Production;Adv. Sci., 2018;5: 1700772.

[11] C. Zhu, A.-L. Wang, W. Xiao, D. Chao, X. Zhang, T. Nguyen Huy, S. Chen, J. Kang, X. Wang, J. Ding, J. Wang, H. Zhang, H.J. Fan, In Situ Grown Epitaxial Heterojunction Exhibits High-Performance Electrocatalytic Water Splitting;Adv. Mater., 2018;30: 1705516.

[12] Z. Chen, D. Cummins, B.N. Reinecke, E. Clark, M.K. Sunkara, T.F. Jaramillo, Core-shell MoO_3-MoS_2 Nanowires for Hydrogen Evolution: A Functional Design for Electrocatalytic Materials;Nano Letters, 2011;11: 4168-75.

[13] B. Cao, G.M. Veith, J.C. Neuefeind, R.R. Adzic, P.G. Khalifah, Mixed Close-Packed Cobalt Molybdenum Nitrides as Non-noble Metal Electrocatalysts for the Hydrogen Evolution Reaction;J. Am. Chem. Soc., 2013;135: 19186-92.

[14] C. Xiao, S. Li, X. Zhang, D.R. MacFarlane, MnO_2/$MnCo_2O_4$/Ni heterostructure with quadruple hierarchy: a bifunctional electrode architecture for overall urea oxidation;J. Mater. Chem. A, 2017;5: 7825-32.

[15] Z. Cao, T. Zhou, X. Ma, Y. Shen, Q. Deng, W. Zhang, Y. Zhao, Hydrogen Production from Urea Sewage on NiFe-Based Porous Electrocatalysts;ACS Sustainable Chem. Eng, 2020;8: 11007-15.

[16] S. Chen, J. Duan, A. Vasileff, S.Z. Qiao, Size Fractionation of Two-Dimensional Sub-Nanometer Thin Manganese Dioxide Crystals towards Superior Urea Electrocatalytic Conversion;Angew.Chem.Int.Ed, 2016;55: 3804-8.

[17] J. Fan, Y. Dou, R. Jiang, K. Du, B. Deng, D. Wang, Electro-synthesis of tungsten carbide containing catalysts in molten salt for efficiently electrolytic hydrogen generation assisted by urea oxidation;Int. J. Hydrogen Energy, 2021;46: 14932-43.